Journal of Inflammation Research

Dovepress
Taylor & Francis Group

Open Access Full Text Article

ORIGINAL RESEARCH

Comparative Efficacy of Coral Calcium Carried Hydrogen versus Dexamethasone in a Mouse Model of Allergic Contact Dermatitis

Gaoxiang Huang[1,*], Dongmei Wei[2,*], Wei Zhao[3], Hao Xu[4], Yankang Wang[2], Xinyao Fu[2], Ye Yang[2], Rong Li[2], Xuzhen Wang[5], Kai Zhou[6], Jing Luan[1,2]

[1]Department of Pathology and Organ Transplantation, Clinical Research Center, The 924th Hospital of the Chinese People's Liberation Army Joint Logistic Support Force, Guilin, Guangxi, People's Republic of China; [2]Shaanxi Key Laboratory of Brain Disorders & Institute of Basic and Translational Medicine, Xi'an Medical University, Xi'an, Shaanxi, People's Republic of China; [3]Department of Medical Logistics, The 924th Hospital of the Chinese People's Liberation Army Joint Logistic Support Force, Guilin, Guangxi, People's Republic of China; [4]Institution of Basic Medical Science, Xi'an Medical University, Xi'an, Shaanxi, People's Republic of China; [5]Rizhao Life Valley Biotechnology Development Co., Ltd, Rizhao, Shandong, People's Republic of China; [6]Department of Otolaryngology, Xi'an No.3 Hospital, The Affiliated Hospital of Northwest University, Xi'an, Shaanxi, People's Republic of China

*These authors contributed equally to this work

Correspondence: Jing Luan, Shaanxi Key Laboratory of Brain Disorders & Institute of Basic and Translational Medicine, Xi'an Medical University, Xi'an, Shaanxi, 710021, People's Republic of China, Email 15619239851@163.com; Kai Zhou Department of Otolaryngology, Xi'an No. 3 Hospital, The Affiliated Hospital of Northwest University, Xi'an, Shaanxi, 710018, People's Republic of China, Email cakerye@163.com

Introduction: Allergic contact dermatitis (ACD) is a common T cell-mediated delayed hypersensitivity reaction characterized by chronic skin inflammation. Coral calcium carried hydrogen (CCH), a novel solid-phase hydrogen carrier, enables sustained hydrogen release and demonstrates superior stability compared to conventional hydrogen delivery methods. However, its therapeutic potential in ACD remains unexplored.

Methods: ACD was induced in female BALB/c mice (8-week-old) using 2,4-dinitrochlorobenzene (DNCB). Mice were divided into four groups: Control, DNCB model, CCH-treated (oral CCH), and dexamethasone (DEX)-treated (oral DEX). Disease severity was assessed through dermatitis scores, scratching frequency, spleen coefficient, and histopathological analysis. Serum cytokine levels and peripheral blood immune cell profiles were evaluated to elucidate the underlying mechanisms.

Results: CCH treatment significantly ameliorated ACD symptoms, comparable to DEX, as evidenced by reduced dermatitis scores, scratching behavior, and spleen enlargement. Histologically, CCH promoted ulcer healing and more effectively suppressed epidermal hyperplasia and skin inflammation than DEX. Mechanistically, CCH selectively reduced serum IgE and IL-17 levels while decreasing lymphocyte counts and proportions. In contrast, DEX primarily inhibited monocytes and neutrophils.

Conclusion: CCH exerts its therapeutic effects by modulating lymphocyte-mediated immune responses and suppressing pro-inflammatory cytokines, offering a promising therapeutic alternative with efficacy comparable to glucocorticoids.

Keywords: allergic contact dermatitis, coral calcium carried hydrogen, anti-inflammatory effects, lymphocytes

Introduction

Allergic contact dermatitis (ACD) is a T cell-mediated delayed hypersensitivity reaction triggered by cutaneous exposure to contact allergens.[1] Clinical manifestations typically present as chronic eczematous lesions characterized by erythema, edema, xerosis and intense pruritus, often persisting beyond acute exposure phases.[2] The global prevalence of ACD has risen significantly, particularly among pediatric populations, with contemporary cases demonstrating more complex immunopathological mechanisms and severe clinical progression refractory to conventional therapies.[3]

The current therapeutic paradigm for ACD comprises three principal interventions: complete allergen avoidance, topical corticosteroid therapy and adjuvant oral antihistamines.[4] Targeted immunomodulation with topical calcineurin

https://doi.org/10.2147/JIR.S571870
Received: 6 October 2025
Accepted: 4 February 2026
Published: 12 February 2026

inhibitors suppressing T-cell activation, combined with narrow-band UVB phototherapy to modulate cutaneous immune responses, constitutes an alternative therapeutic approach.[5] However, current therapeutic strategies confront three predominant clinical limitations including the impracticality of systemic allergen avoidance due to ubiquitous environmental sensitizers, the risk of cutaneous atrophy from prolonged high-potency corticosteroid use, and the limited efficacy of H1-antagonists against neuroimmune-mediated pruritus.[6] Critically, existing therapeutic modalities focus on symptomatic management while failing to address the core pathogenetic mechanisms of immunological memory formation. Therefore, developing innovative therapeutic strategies that address both acute symptom control and long-term disease modification, particularly through sustained anti-inflammatory mechanisms without corticosteroid-dependent effects, represents a critical unmet need in ACD management. Current research endeavors are investigating diverse therapeutic strategies, including biologics targeting specific immune pathways, plant-derived bioactive agents with multimodal mechanisms, and novel small-molecule inhibitors, to develop alternatives with enhanced safety profiles and sustained efficacy in ACD management.[7]

Emerging evidences from mechanistic investigations have established molecular hydrogen as a novel therapeutic agent with multimodal biological effects. It has been reported that molecular hydrogen exerts cytoprotective effects in vivo through targeted modulation of pathological progression, via orchestrated mechanisms involving: scavenging reactive oxygen species (ROS) through selective antioxidant activity,[8] suppressing inflammatory cascades,[9] activating longevity pathways,[10] and enhancing lysosomal autophagy flux.[11] Accumulating preclinical and clinical evidences indicate molecular hydrogen exerts cytoprotective effects. Molecular hydrogen has emerged as a novel therapeutic candidate owing to its unique capacity to permeate cellular membranes within seconds and mediate targeted biological responses, coupled with a favorable safety profile.[9]

Coral calcium carried hydrogen (CCH), synthesized from marine-derived coral calcium, constitutes an innovative solid-state molecular hydrogen carrier system. Under high-temperature, high-pressure anoxic conditions, hydrogen undergoes dielectric polarization within the plasma phase, resulting in the formation of negatively charged hydride ions (H^-). These H^- are incorporated into the crystal lattice and micropores of calcium carbonate and magnesium during their polarized and ionized states, creating stable negative hydrogen ionophores at room temperature. Under low-oxygen conditions in biological systems, CCH reacts with water to form Ca^{2+}, Mg^{2+}, and H^- while continuously releasing hydrogen.[12–14] Growing preclinical evidences highlight its multi-organ protective effects mediated primarily through anti-oxidative and anti-inflammatory actions. For instance, CCH supplementation had been shown to prevent high-fat diet-induced hepatic steatosis in rats by improving mitochondrial function and activating Phase II detoxification enzymes.[14] In a model of chronic hypoxia, CCH attenuated bone degeneration and multi-organ damage, potentially via modulating the gut microbiota and alleviating systemic inflammation.[15] Furthermore, CCH exerted a gastroprotective effect by reducing pro-inflammatory cytokine expression and enhancing antioxidative enzyme levels in peptic ulcer disease.[16] More directly relevant to cellular stress mitigation, Li et al demonstrated that CCH functioned as a hydrogen donor to activate the Trx2/Myo19/phospho-Drp1 signaling axis, preserving mitochondrial homeostasis in alveolar type II epithelial cells through ROS scavenging, which attenuated oxidative stress-mediated acute lung injury in respiratory distress syndrome models.[17] However, its therapeutic potential and mechanism of action in ACD remain completely unexplored. ROS plays a pivotal role in the pathogenesis of ACD by facilitating inflammatory responses, modulating cellular signal transduction, inducing oxidative stress, activating immune cells, and compromising skin barrier integrity. Consequently, it is posited that CCH holds a significant promise for treating ACD. We hypothesize that CCH administration will ameliorate ACD primarily through the suppression of inflammatory and immune responses. Herein, we aim to investigate the therapeutic effects and underlying mechanism of CCH in a 2,4-dinitrochlorobenzene (DNCB)-induced mouse model of ACD. Our findings are expected to provide preclinical evidence supporting its potential clinical application.

Materials and Methods

Experimental Animals

Female BALB/c mice (8-week-old, 20–22 g) were purchased from Hua Fukang Biotechnology Co., Ltd (Beijing, China). Mice were maintained in ventilated microisolator cages with a 7-day acclimation period (12:12 light-dark cycle, 22±1°C,

50–60% humidity) within the specific pathogen-free facility of the Laboratory Animal Center at Xi'an Medical University, and provided standard chow and tap water ad libitum. All experimental protocols were approved by the Institutional Ethics Committee on Animal Use of Xi'an Medical University (Approval No. XYLS2021208), and all procedures were conducted in accordance with the committee's guidelines and regulations. No unexpected adverse events occurred in this study.

Chemicals and Reagents

DNCB (Cat# 16051) and dexamethasone (DEX, Cat# A13449) were purchased from Sigma-Aldrich (St. Louis, MO, USA). Acetone (HPLC grade, Cat# 400100025) and olive oil (Cat# 416540025) were purchased from Thermo Fisher Scientific (Shanghai, China). CCH was kindly provided by Rizhao Life Valley Biotechnology Development Co., Ltd. (Shandong, China). CCH and DEX were dissolved in ultrapure water. DNCB was prepared in acetone/olive oil (3:1 v/v) and freshly prepared before use.

Establishment of the ACD Animal Model and Experimental Design

Following a 7-day acclimatization period, dorsal hair was removed prior to model induction. The ACD model was established through sequential chemical exposure: 1% DNCB in acetone/olive oil (3:1 v/v) was topically applied to shaved dorsal skin daily on Days 1–3 (sensitization phase), followed by 0.4% DNCB applications daily from Days 8–13. Pharmacological interventions (CCH and DEX) were administered daily via oral gavage from Day 1 until experimental endpoint. On day 14 post-intervention, the mice underwent terminal anesthesia via intraperitoneal injection of sodium pentobarbital (40 mg/kg), followed by systematic collection of dorsal skin biopsies, splenic parenchyma, and peripheral venous blood for subsequent analyses. Following terminal anesthesia, the mice were euthanized by cervical dislocation at the experimental endpoint.

A total of thirty-two BALB/c mice were randomly allocated to four groups using a computer-generated random number sequence (Excel RAND function). Control group: Topical acetone-olive oil (3:1 v/v) + oral saline daily. DNCB model group: Sensitized with 1% DNCB (days 1–3), challenged with 0.4% DNCB (days 8–13) + oral saline daily. CCH group: DNCB stimulation + oral CCH daily (5 mg/mL, 50 mg/kg/day). DEX group: DNCB stimulation + oral DEX daily (0.2 mg/mL, 2 mg/kg/day). Each mouse received an individual drug intervention (experimental unit= single animal; N=8 mice per group). Sample size was determined by power analysis (effect size Cohen's d=1.70; α=0.05, two-tailed; power=0.80) based on a pilot study evaluating the primary outcomes: dermatitis scores and scratching frequency. Experimenters were blinded to group identity (drugs were coded as A/B/C/D/E) during data collection and analysis. All animals and data points were included in the analysis.

Detection of the Dissolved Hydrogen in CCH Solution

Following preparation of CCH solutions with varying concentration gradients, dissolved hydrogen levels were quantified at predetermined intervals (2, 4, 6, 8, 10, 12, 24, 48 hours post-preparation) using a calibrated portable hydrogen analyzer (ENH-2000, Trustlex, Japan). Measurements at each time point were based on three independent replicate experiments under ambient temperature (25±1°C) with sensor calibration performed according to manufacturer specifications.

Monitoring of Body Weight in Mice

Longitudinal body weight measurements were obtained at baseline (day 1 post-modeling) and endpoint (day 14 post-modeling). Weight trajectory analysis served as a surrogate marker for evaluating both modeling stress and potential CCH-associated toxicity.

Measurement of Dermatitis Scores

A double-blind scoring was performed to determine the dermatitis scores of mice according to the severity of manifestations on the dorsal skin of mice. On the indicated days (D5, D7, D13) post-modeling, dermatitis severity was blindly assessed by two investigators using a published scoring system based on dorsal skin manifestations.[18] Three macroscopic features (erythema/hemorrhage, scratches/erosions, scaling/mossy changes) were graded 0–4 based on

affected dorsal skin area: 0 (absent), 1 (<10%), 2 (10–39%), 3 (40–75%), and 4 (>75%). In addition, skin edema severity was graded 0–4: 4 (marked swelling with dark erythema); 3 (moderate swelling, light erythema, and xerosis); 2 (textural irregularity with hyperpigmentation); 1 (smooth texture comparable to controls); 0 (no pathological changes). The total dermatitis scores were derived from the cumulative sum of all macroscopic feature evaluations.

Measurement of Scratching Behavior

On the indicated days (D7, D13) post-modeling, mice were individually placed in plastic cages for 1 hour to acclimate. Dorsal scratching behavior was recorded for 10 minutes, with one scratch defined as a continuous hind paw movement directed at the dorsal skin. Three independent observers counted the total scratches per mouse, and final values were averaged.

Histological Analysis

At study termination, dorsal skin specimens (≈1 cm^2) were excised from lesioned areas using sterile surgical scissors. Tissues were fixed in 4% paraformaldehyde (24 h), paraffin-embedded, and sectioned at 5 μm for hematoxylin and eosin (H&E) staining.

Quantification of ulcer depth and epidermal thickness was performed using digital image analysis software (CaseViewer, 3DHISTECH, Hungary). Ulcer depth was defined and measured as the minimal vertical distance from the base of the ulceration to the underlying subdermal muscle layer. Epidermal thickness was quantified as the vertical distance from the basal layer to the stratum corneum. Three measurements were taken and averaged in non-overlapping interfollicular regions for each sample.

Inflammatory cell infiltration was assessed by a blinded pathologist under a light microscope. For each H&E-stained section, inflammatory cells (primarily lymphocytes, neutrophils, and monocytes/macrophages) were identified based on morphological criteria and manually counted in five randomly selected, non-overlapping high-power fields (HPF, ×200 magnification). The total cell count per HPF was then calculated for each sample.

Cytokines Assay

Peripheral blood samples were collected via orbital puncture and centrifuged (3000 × g, 15 min) to isolate plasma, which was stored at −20°C until assay. Serum concentrations of TNF-α, IL-4, IL-17, and IgE were quantified using commercial ELISA kits (MultiSciences Biotech, China) following manufacturer protocols.

Counting of Peripheral Blood Cells in Mice

Heparinized blood collected via orbital puncture was gently inverted to prevent bubble formation. Samples were diluted with PBS (1:10) to meet the ProCyte Dx Hematology Analyzer (IDEXX, USA) detection range. Complete blood counts were performed per manufacturer's protocol, with quality control verification using standard calibration particles before each run.

Statistical Analysis

Data analysis was performed using GraphPad Prism 8.0 (GraphPad Software, USA). One-way or two-way ANOVA with SNK-q multiple comparison test was employed for group comparisons. Normality was assessed by Shapiro–Wilk test (α=0.05). For non-normal data, log-transformation was applied. Results are presented as mean ± standard deviation (SD), with statistical significance set at $P < 0.05$.

Results

Dose Selection of CCH Solution

As illustrated in Figure 1, dissolved hydrogen concentrations were measured at specified time points in CCH solutions of varying concentrations. The hydrogen concentration in CCH solution peaked within 2 hours post-preparation and remained stable at this elevated level before declining precipitously after 24 hours. Trace amounts of dissolved hydrogen

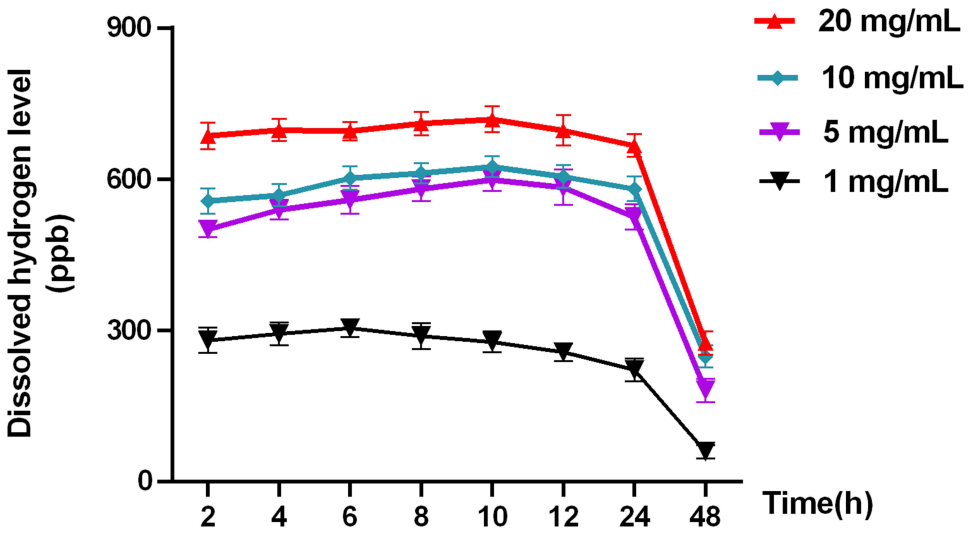

Figure 1 Dissolved hydrogen concentration kinetics and optimal dose determination in CCH solutions. Hydrogen release profiles were measured at 2-hour intervals for four CCH concentrations (1, 5, 10, and 20 mg/mL) and data are presented as the mean ± SD.

persisted up to 48 hours. There were no significant differences in dissolved hydrogen concentrations between 5 mg/mL and 10 mg/mL CCH solutions. Although the 20 mg/mL CCH solution exhibited higher hydrogen concentrations, its turbid appearance precluded clinical applicability. Consequently, based on these data, we determined that 5 mg/mL CCH administered once daily represents the optimal dosage regimen for subsequent animal studies.

Effects of CCH and DEX on the Symptoms and Inflammation Response

On days 4–5 following DNCB stimulation, the dorsal skin of mice began exhibiting dermatitis symptoms, including varying degrees of xerosis, silvery-gray scaling, papules, and erythema. Repeated 0.4% DNCB stimulation from day 8 onward sustained the inflammatory response, leading to scab formation and progressive lesion aggravation, with underlying tissues displaying pronounced erythema and edema (Figure 2A).

Dermatitis scores were 0 (control) and ~9 (DNCB group), respectively. Skin severity was ameliorated in the DEX group compared to the DNCB group ($P < 0.01$). The CCH group exhibited a significantly lower dermatitis score than the DNCB group ($P < 0.001$, Figure 2B).

Frequent scratching behavior was observed in the DNCB group. Compared to the DNCB group, scratching frequency decreased by 33.23% in the CCH group ($P < 0.05$) and by 39.1% in the DEX group ($P < 0.05$), respectively (Figure 2C).

Body weights were monitored on days 1 and 14. While all groups exhibited marginal weight gain, CCH treatment did not significantly alter body weight, suggesting an absence of adverse metabolic effects. DEX slightly attenuated weight gain, though intergroup differences were not statistically significant (Figure 2D).

The spleen coefficient (spleen to body weight ratio), an indicator of systemic inflammation and immune activation, was significantly elevated in the DNCB group (0.0116 vs 0.0043 in control group), reflecting pronounced inflammatory responses. Both CCH (0.0074, $P < 0.05$) and DEX (0.0053, $P < 0.01$) treatments suppressed splenomegaly and inflammation (Figure 2E).

Furthermore, to determine whether the effects originated from the hydrogen release rather than the coral calcium matrix itself, we compared symptom severity between DNCB-induced ACD mice treated with oral saline and those treated with oral coral calcium (CC) alone. No statistically significant differences were observed in dermatitis scores, number of scratches, spleen coefficient or weight between the two groups (Supplementary Figure 1A–E).

Effects of CCH and DEX on Histopathological Lesions

H&E staining demonstrated significant pathological alterations in the DNCB group compared to controls, including ulceration, hyperkeratosis, epidermal hyperplasia, partial loss of skin appendages, and severe skin inflammatory

https://doi.org/10.2147/JIR.S571870

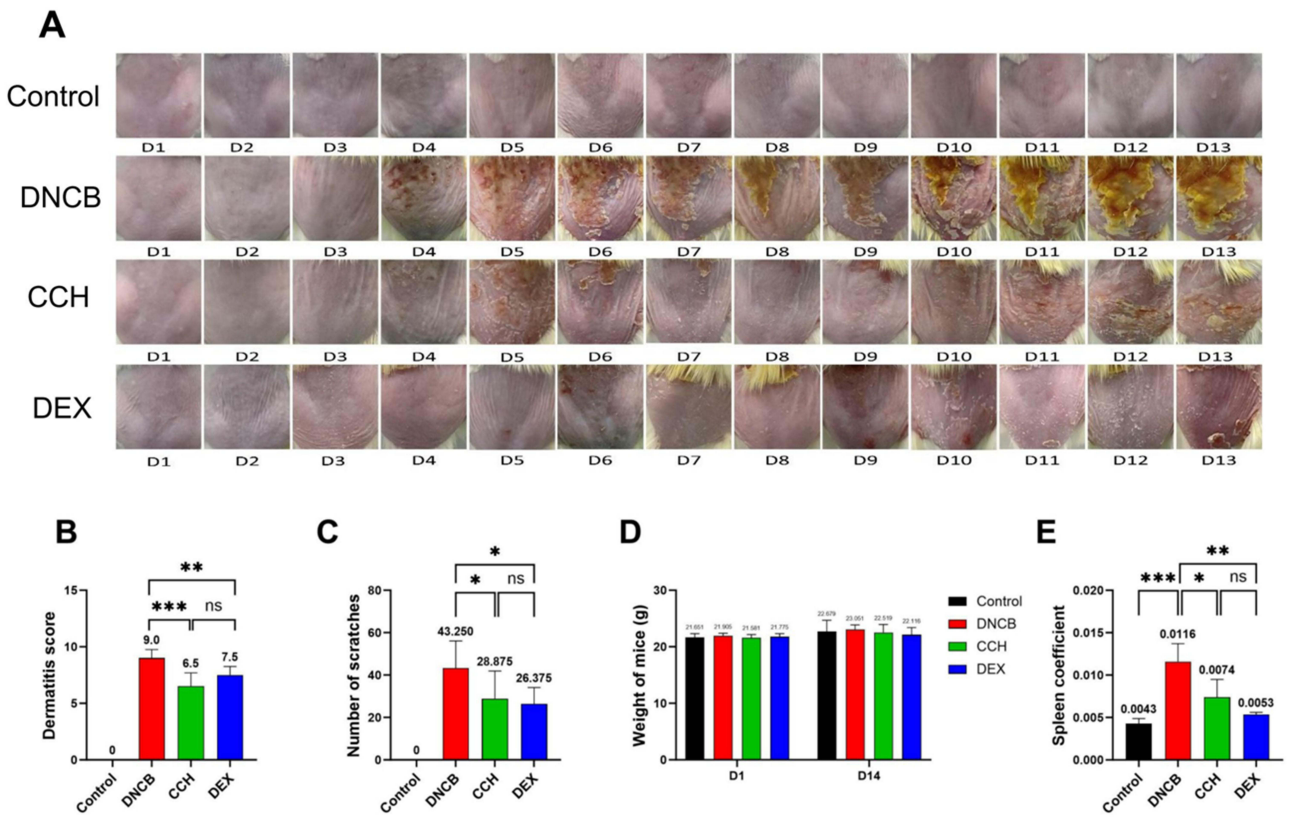

Figure 2 Effects of CCH and DEX on the symptoms and inflammation response in ACD mice. (**A**) Representative lesions from Day 1 to Day 13 in each group. Dermatitis scores (**B**) and scratching frequency (**C**) of mice in each group were assessed on day 7 post-modeling. (**D**) Weight changes of mice in each group. Mice were weighed on day 1 and day 14. (**E**) Spleen coefficient of mice was assessed on day 14 post-modeling. After the mice were anesthetized, the spleens were removed and weighed. The spleen coefficient was calculated by dividing the spleen weight by the body weight. N=8 per group. Data represent mean ± SD. *$P < 0.05$, **$P < 0.01$, and ***$P < 0.001$.

infiltration (Figure 3A and C). Skin ulceration in the DNCB group was characterized by necrotic tissue, inflammatory exudates, and full-thickness epidermal defects (Figure 3A). Both CCH and DEX treatments substantially reduced ulcer depth (measured as the minimal distance from the ulcer base to the subdermal muscle layer), with reductions of 32% ($P < 0.001$) and 53% ($P < 0.001$), respectively, relative to the DNCB group (Figure 3B). Notably, DEX outperformed CCH in ulcer improvement ($P < 0.0001$).

The DNCB group exhibited mossy skin morphology due to keratinocyte proliferation and stratum corneum thickening (Figure 3C). Epidermal thickness increased 3.8-fold versus controls ($P < 0.0001$), with CCH treatment significantly attenuating this hyperplasia by 28% ($P < 0.001$). In contrast, DEX showed no significant effect on epidermal thickness (Figure 3D). However, DEX-treated mice developed unique lesions, including hyperkeratosis, parakeratosis, and follicular keratosis, which were rare in other groups (Figure 3C). No intergroup differences in dermal thickness were observed (data not shown).

The DNCB group displayed marked inflammatory cell infiltration involving the epidermis and dermis versus controls ($P < 0.0001$; Figure 3E and F). Both CCH ($P < 0.05$) and DEX ($P = 0.43$) reduced the infiltration, though CCH exhibited superior efficacy.

Effects of CCH and DEX on Serum Cytokine Profiles

Key cytokines associated with ACD pathogenesis were quantified, including Th1-derived TNF-α, Th2-derived IL-4, Th17-derived IL-17, and plasma cell-derived IgE. Serum analysis revealed significantly elevated IgE levels in the DNCB group compared to controls ($P < 0.0001$). Both CCH and DEX treatments substantially reduced IgE levels by 47.5% ($P < 0.01$) and 49.9% ($P < 0.01$), respectively (Figure 4A). While the DNCB group exhibited a three-fold increase in IL-17 levels versus controls, both treatment groups showed reductions (CCH: 42.4%; DEX: 33.4%), though these changes did not reach statistical significance (Figure 4B). No significant alterations were observed in TNF-α or IL-4 levels (data not shown).

https://doi.org/10.2147/JIR.S571870

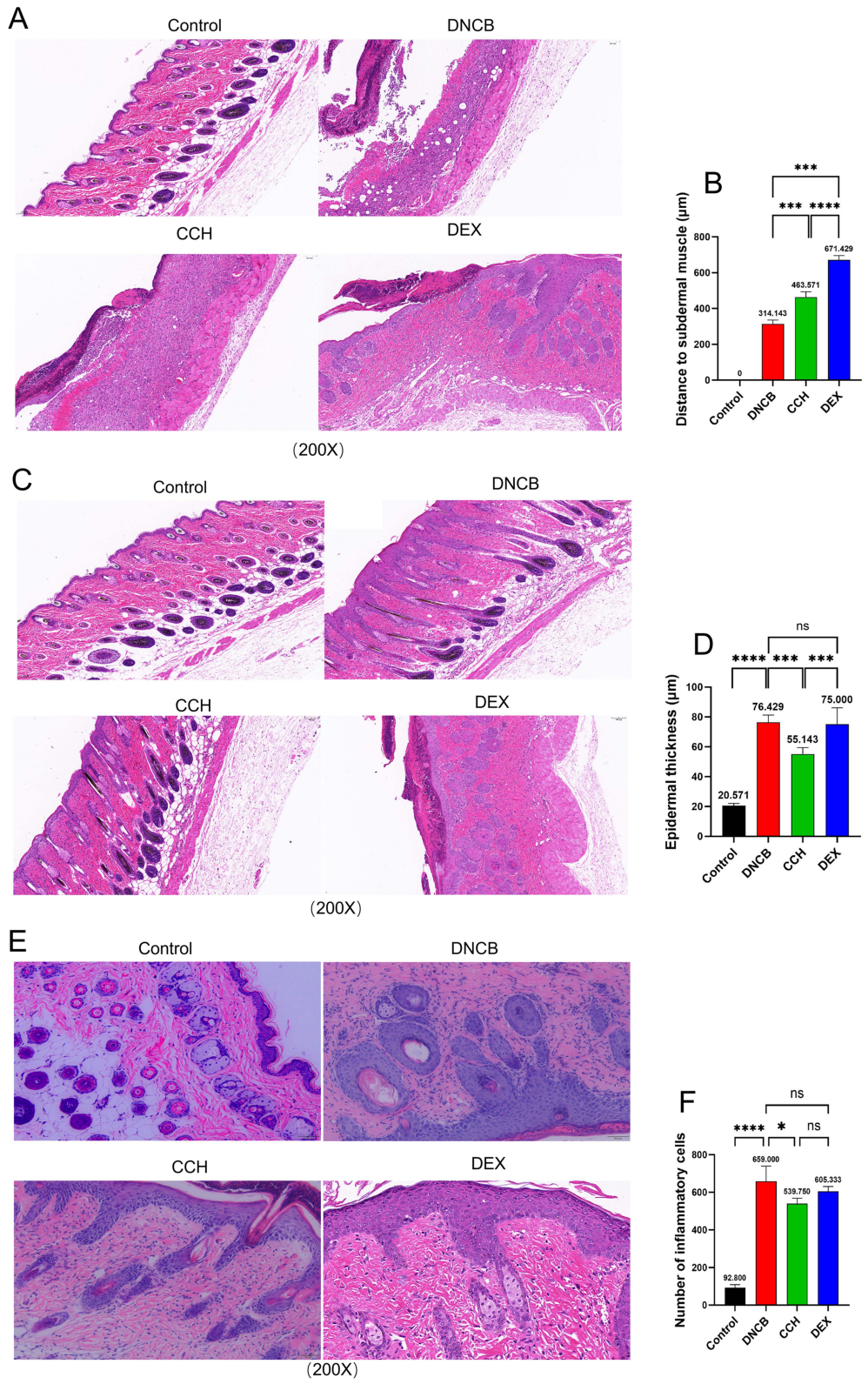

Figure 3 Therapeutic effects of CCH and DEX on the pathological lesions in ACD mice. (**A**) Representative H&E-stained skin tissue sections (×200 magnification) demonstrating dermal ulceration. (**B**) Quantitative analysis of ulcerous depth, measured as the minimal vertical distance from the ulceration base to subdermal muscle layer. (**C**) Histopathological presentation of epidermal hyperplasia (×200 magnification). (**D**) Epidermal thickness quantification. (**E**) Histopathological presentation of inflammation involving the epidermis and dermis (×200 magnification). (**F**) Inflammatory cell infiltration counts in the epidermal and dermal tissue. N=8 per group. Data represent mean ± SD. **P* < 0.05, ****P* < 0.001, and *****P* < 0.0001.

https://doi.org/10.2147/JIR.S571870

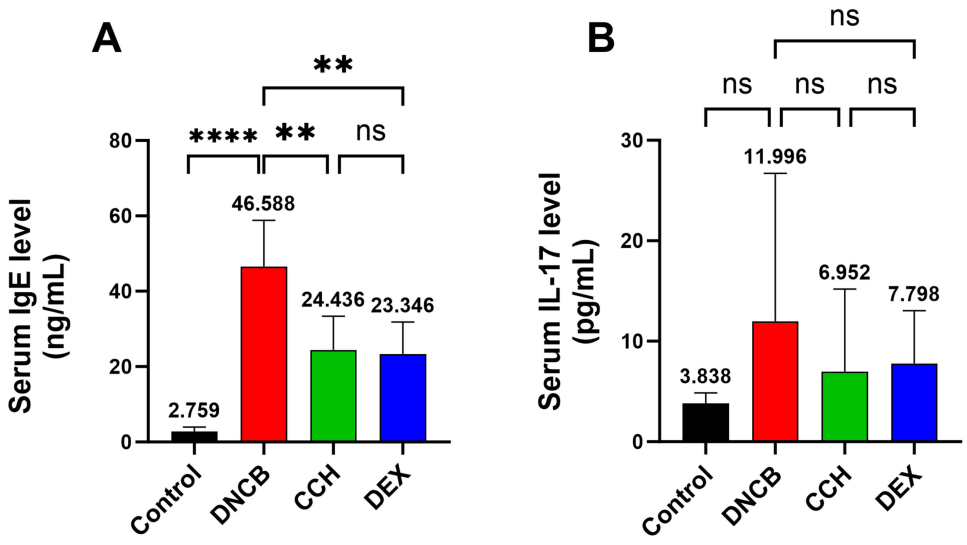

Figure 4 Effects of CCH and DEX on serum cytokine profiles in ACD mice. Serum IgE (**A**) and IL-17 (**B**) levels were measured. N=8 per group. Data represent mean ± SD. $^{**}P < 0.01$, and $^{****}P < 0.0001$.

Effects of CCH and DEX on Peripheral Blood Immune Cell Profiles

To elucidate the immunomodulatory mechanisms of CCH and DEX, we analyzed peripheral blood immune cell populations in ACD mice. DNCB-stimulated mice exhibited significantly elevated lymphocyte counts compared to controls ($P < 0.01$; Figure 5A), though lymphocyte percentages remained unchanged (Figure 5D).

Notably, while DEX treatment further increased absolute lymphocyte numbers versus the DNCB group ($P < 0.01$), CCH administration showed a tendency to reduce both lymphocyte proportion ($P = 0.1791$) and absolute count ($P = 0.0854$). Importantly, CCH demonstrated significantly stronger inhibition than DEX on both lymphocyte parameters (absolute count: $P < 0.0001$; proportion: $P < 0.01$; Figure 5A and D).

DNCB stimulation also increased monocyte and neutrophil numbers and proportions versus controls (Figure 5B, C, E and F). DEX treatment showed a clear downward trend in these myeloid populations, though the changes did not reach statistical significance. In contrast, CCH had minimal effects on monocyte or neutrophil parameters compared to the DNCB group.

Discussion

Molecular hydrogen has emerged as a promising therapeutic agent due to its diverse biological properties, including antioxidative, anti-inflammatory, and anti-aging effects.[19–22] However, its clinical application is limited by physicochemical challenges, such as rapid diffusion due to low molecular weight, poor aqueous solubility and transient biological activity. Conventional hydrogen delivery systems (eg, hydrogen-rich water/saline) require specialized aluminum containers, yet still suffer from rapid hydrogen dissipation upon opening. However, CCH overcomes these limitations by enabling sustained hydrogen release in vivo.[14–17]

In this study, oral CCH effectively alleviated DNCB-induced ACD in mice, with efficacy comparable to DEX. CCH significantly improved symptoms, including dermatitis scores, scratching behavior, and systemic inflammation reflected by spleen coefficient. Histopathological assessment further revealed that CCH promoted ulcer healing and, more effectively than DEX, suppressed epidermal hyperplasia and skin inflammation. Mechanistically, CCH selectively lowered serum IgE and showed a trend in reducing IL-17, paralleling its specific suppression of lymphocytes. In contrast, DEX primarily affected monocytes and neutrophils.

To our knowledge, CCH itself has not been previously studied in dermatological diseases, its investigation in ACD is strongly supported by two key aspects of its composition and the established biological effects of its active component. Firstly, CCH is a unique solid-phase carrier designed for sustained release of hydrogen. The therapeutic potential of hydrogen

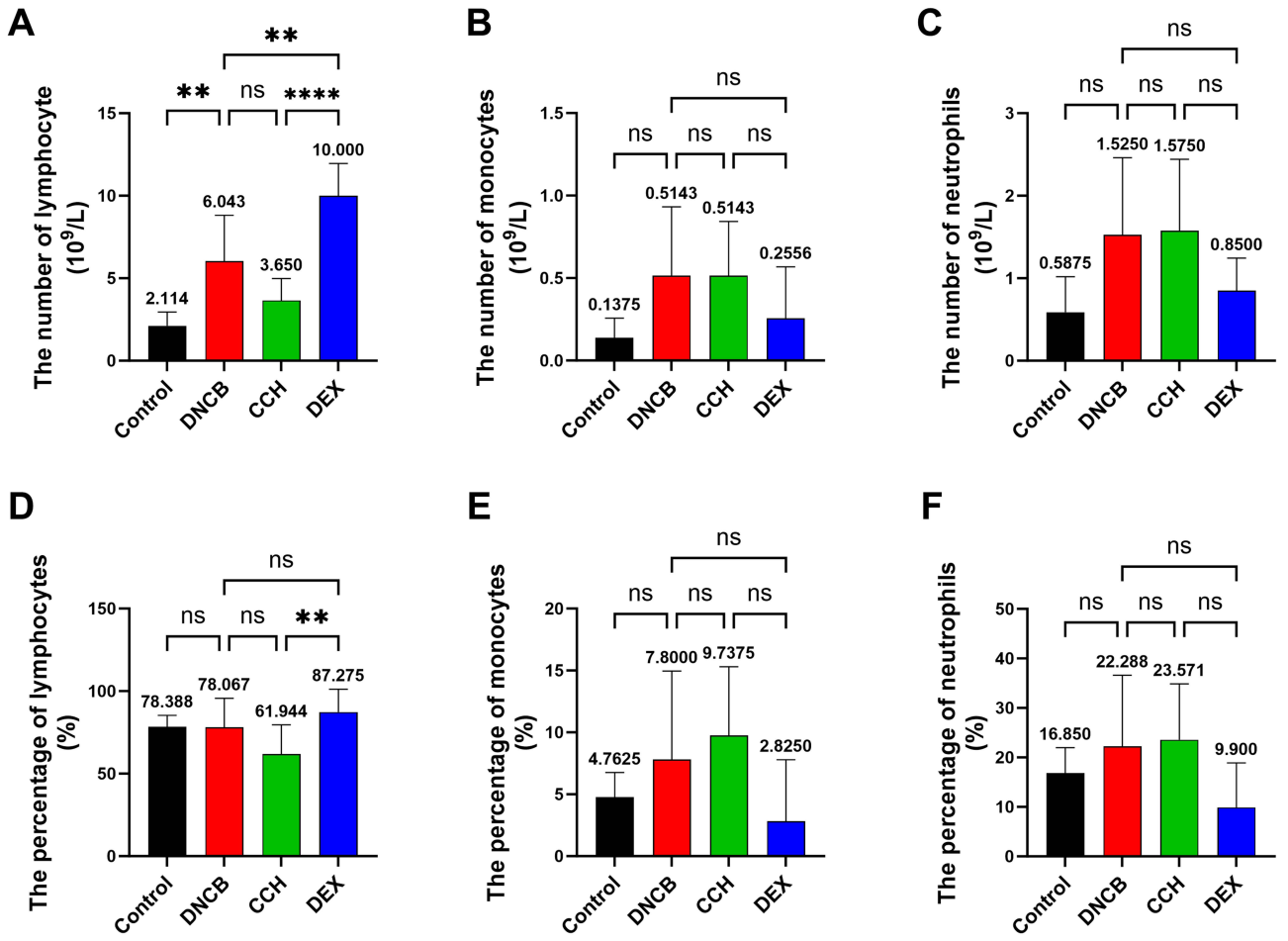

Figure 5 Effects of CCH and DEX on peripheral blood immune cells in ACD mice. (**A**–**C**) Absolute counts of (**A**) lymphocytes (T and B cells), (**B**) monocytes, and (**C**) neutrophils. (**D**–**F**) Proportional distribution of (**D**) lymphocytes (T and B cells), (**E**) monocytes, and (**F**) neutrophils among total leukocytes. N=8 per group. Data represent mean ± SD. $^{**}P < 0.01$, and $^{****}P < 0.0001$.

in skin inflammation is underpinned by its well-documented anti-oxidative and anti-inflammatory properties, which are highly relevant to the pathophysiology of ACD. This rationale is supported by previous studies indicating the beneficial effects of hydrogen in other dermatological diseases. For instance, hydrogen-rich baths have been shown to ameliorate symptoms in a mouse model of imiquimod-induced psoriasis, and hydrogen has demonstrated a protective effect on hydrogen peroxide-injured human melanocytes, suggesting its potential as a therapeutic agent for conditions like vitiligo.[23,24] Secondly, the solid matrix of CCH is derived from coral calcium, a nutritional supplement rich in calcium and essential minerals that has been associated with bone loss protection.[25] However, our Supplementary Data (Supplementary Figure 1) confirmed that oral administration of coral calcium alone did not alleviate ACD symptoms such as dermatitis scores, scratching frequency and spleen coefficient, indicating that the observed therapeutic efficacy is primarily attributable to the sustained release of hydrogen from the CCH complex, rather than to the calcium carrier. Therefore, our work translates the known mechanistic benefits of hydrogen into a novel, convenient and effective oral solid formulation for managing ACD.

Oral administration of CCH significantly ameliorated dermatitis symptoms and reduced pro-inflammatory cytokines with comparable efficacy to DEX in DNCB-induced ACD mice. However, their effects on histopathological features revealed distinct profiles. While CCH more effectively suppressed epidermal hyperplasia and inflammatory cell infiltration, DEX showed superior efficacy in promoting ulcer healing. Collectively, CCH demonstrated comparable anti-inflammatory efficacy to DEX, a potent glucocorticoid standard for inflammatory diseases, suggesting a significant therapeutic potential of CCH in ACD management. As a potent glucocorticoid, DEX exerted broad anti-inflammatory and immunosuppressive effects through multiple pharmacological

https://doi.org/10.2147/JIR.S571870

mechanisms.[26] Notably, while achieving similar therapeutic outcomes, CCH administration avoided the weight fluctuations associated with DEX treatment, suggesting superior safety profile.

Mechanistically, CCH and DEX displayed the divergent immunomodulatory profiles. CCH preferentially targeted the adaptive immune system, as evidenced by suppression of lymphocyte counts and proportions, coupled with selective reduction in lymphocyte-related cytokines (IgE and IL-17). This sustained efficacy likely resulted from CCH's unique capacity for prolonged hydrogen release in vivo. Speculatively, the sustained hydrogen release from CCH likely mitigated ACD by alleviating oxidative stress via selective ROS scavenging.[17,27–29] This reduction in oxidative stress could concurrently inhibit ROS-sensitive pro-inflammatory signaling NLRP3 inflammasome and NF-κB activation and activated endogenous protective pathways such as Nrf2 signaling. Together, these signaling suppressed lymphocyte proliferation and activation, inhibited the differentiation of pro-inflammatory subsets like Th17 cells, and reduced the production of downstream effectors including IL-17 and IgE.[27–30] In contrast, DEX, as a broad-spectrum glucocorticoid, primarily exerted its influence on the innate immune compartment, showing a clear inhibitory trend on monocytes and neutrophils. This aligned with the canonical mechanism of glucocorticoids, which potently suppressed the recruitment and pro-inflammatory functions of myeloid cells.[26] Because the DNCB-induced ACD pathology involved in innate immune cells and pathogenic T cells that formed an interdependent loop, inhibiting either the innate immune activation targeted by DEX or the subsequent pathogenic T-cell expansion targeted by CCH could disrupt the loop and alleviated the disease. This mechanistic divergence highlights a potential therapeutic advantage for CCH. A lymphocyte-focused approach may offer a more targeted strategy with a potentially superior safety profile, possibly avoiding the broader immunosuppression and metabolic disturbances associated with systemic glucocorticoid therapy that acts heavily on innate immunity.

This study, while providing compelling evidence for the efficacy of CCH in a murine model of ACD, has several inherent limitations that warrant consideration. The preclinical nature of our work means the findings need to be validated in other animal models and, crucially, in clinical trials to establish their translational relevance. A key unresolved question is the precise molecular mechanism underlying CCH's selective suppression of lymphocytes. Future investigations employing transcriptomic or proteomic analyses of isolated lymphocyte populations could illuminate the specific signaling pathways modulated by CCH-derived hydrogen. Furthermore, the long-term safety profile of chronic CCH administration requires more comprehensive evaluation.

In conclusion, our findings position CCH as a promising therapeutic alternative for ACD by modulating lymphocyte-mediated immune responses and suppressing pro-inflammatory cytokines, combining DEX-comparable efficacy with improved safety.

Declaration of Generative AI in Scientific Writing

The article did not employ any AI technology.

Data Sharing Statement

The data that support the findings of this study are available from the corresponding author upon reasonable request.

Ethical Approval

All animal experimental procedures were conducted in strict compliance with institutional and national guidelines for the care and use of laboratory animals. The study protocol was reviewed and approved by the Institutional Animal Care and Use Committee of Xi'an Medical University (Approval No. XYLS2021208). All efforts were made to minimize animal suffering and reduce the number of animals used, in accordance with the ARRIVE guidelines.

Acknowledgments

The authors thank the Academician Workstation of Chen Zhi-nan in Xi'an city and the Rizhao Life Valley Biotechnology Development Co., Ltd for providing technical support.

Author Contributions

Gaoxiang Huang; Conceptualization, Formal analysis, Funding acquisition, Investigation, Writing - original draft. Dongmei Wei; Formal analysis, Investigation, Methodology, Validation, Writing - original draft. Wei Zhao; Methodology, Software. Hao Xu; Data curation, Methodology, Validation. Yankang Wang; Data curation, Investigation, Methodology. Xinyao Fu; Data curation, Investigation, Methodology, Software. Ye Yang; Investigation, Methodology, Software. Rong Li; Methodology, Validation. Xuzhen Wang; Methodology, Resources. Kai Zhou; Conceptualization, Funding acquisition, Project administration, Writing - review & editing. Jing Luan; Conceptualization, Funding acquisition, Methodology, Project administration, Supervision, Writing - review & editing. All authors took part in drafting, revising or critically reviewing the article; gave final approval of the version to be published; have agreed on the journal to which the article has been submitted; and agree to be accountable for all aspects of the work.

Funding

This study was supported by the Natural Science Foundation of China (32260239), the Natural Science Basic Research Program of Shaanxi Province (2024JC-YBMS-726, 2020JZ-56), the Key Research and Development Program of Shaanxi Province (2024SF-YBXM-347) and the Program for Science and Technology Innovation Team in Xi'an Medical University (2021TD05).

Disclosure

The corresponding author Jing Luan holds a Chinese invention patent (Patent No. ZL202411256525.1) related to the compound reported in this study. This may constitute a potential conflict of interest regarding the commercial exploitation of the technology. The authors have no other conflicts of interest to declare.

References

1. Adler BL, DeLeo VA. Allergic contact dermatitis. *JAMA Dermatol*. 2021;157(3):364. doi:10.1001/jamadermatol.2020.5639
2. Nassau S, Fonacier L. Allergic contact dermatitis. *Med Clin North Am*. 2020;104(1):61–76. doi:10.1016/j.mcna.2019.08.012
3. Belloni Fortina A, Caroppo F, Tadiotto Cicogna G. Allergic contact dermatitis in children. *Expert Rev Clin Immunol*. 2020;16(6):579–589. doi:10.1080/1744666X.2020.1777858
4. Fonacier L, Uter W, Johansen JD. Recognizing and managing allergic contact dermatitis: focus on major allergens. *J Allergy Clin Immunol Pract*. 2024;12(9):2227–2241. doi:10.1016/j.jaip.2024.04.060
5. Hon KL, Leung AKC, Cheng JWCH, Luk DCK, Leung ASY, Koh MJA. Allergic contact dermatitis in pediatric practice. *Curr Pediatr Rev*. 2024;20(4):478–488. doi:10.2174/1573396320666230626122135
6. Sadrolvaezin A, Pezhman A, Zare I, et al. Systemic allergic contact dermatitis to palladium, platinum, and titanium: mechanisms, clinical manifestations, prevalence, and therapeutic approaches. *MedComm*. 2023;4(6):e386. doi:10.1002/mco2.386
7. Okamoto M, Omori-Miyake M, Kuwahara M, Okabe M, Eguchi M, Yamashita M. The inhibition of glycolysis in T cells by a Jak inhibitor ameliorates the pathogenesis of allergic contact dermatitis in mice. *J Invest Dermatol*. 2023;143(10):1973–1982. doi:10.1016/j.jid.2023.03.1667
8. Kura B, Bagchi AK, Singal PK, et al. Molecular hydrogen: potential in mitigating oxidative-stress-induced radiation injury. *Can J Physiol Pharmacol*. 2019;97(4):287–292. doi:10.1139/cjpp-2018-0604
9. Yin H, Feng Y, Duan Y, Ma S, Guo Z, Wei Y. Hydrogen gas alleviates lipopolysaccharide-induced acute lung injury and inflammatory response in mice. *J Inflamm (Lond)*. 2022;19(1):16. doi:10.1186/s12950-022-00314-x
10. Fu Z, Zhang J, Zhang Y. Role of molecular hydrogen in ageing and ageing-related diseases. *Oxid Med Cell Longev*. 2022;2022:2249749. doi:10.1155/2022/2249749
11. Yao L, Chen H, Wu Q, Xie K. Hydrogen-rich saline alleviates inflammation and apoptosis in myocardial I/R injury via PINK-mediated autophagy. *Int J Mol Med*. 2019;44(3):1048–1062. doi:10.3892/ijmm.2019.4264
12. Li Q, Yu P, Zeng Q, et al. Neuroprotective effect of hydrogen-rich saline in global cerebral ischemia/reperfusion rats: up-regulated Tregs and down-regulated miR-21, miR-210 and NF-κB expression. *Neurochem Res*. 2016;41(10):2655–2665. doi:10.1007/s11064-016-1978-x
13. Ueda Y, Nakajima A, Oikawa T. Hydrogen-related enhancement of in vivo antioxidant ability in the brain of rats fed coral calcium hydride. *Neurochem Res*. 2010;35(10):1510–1515. doi:10.1007/s11064-010-0204-5
14. Hou C, Wang Y, Zhu E, et al. Coral calcium hydride prevents hepatic steatosis in high fat diet-induced obese rats: a potent mitochondrial nutrient and phase II enzyme inducer. *Biochem Pharmacol*. 2016;103:85–97. doi:10.1016/j.bcp.2015.12.020
15. Zhu S, Hao D, Chen Y, et al. Hydrogen intervention attenuates chronic hypoxia-induced bone degeneration and multi-organ damage via modulation of the gut microbiota. *Bone*. 2026;203:117718. doi:10.1016/j.bone.2025.117718
16. Wu HT, Hsieh MT, Ou HY, Chao TH, Tsai LM. The Gastroprotective Effect of Hydrogen-Rich Coral Calcium in a Mouse Model of Peptic Ulcer Disease. *Drug Des Devel Ther*. 2025;19:9845–9851. doi:10.2147/DDDT.S555188
17. Li Q, Ang Y, Qq Z, et al. Coral calcium hydride promotes peripheral mitochondrial division and reduces AT-II cells damage in ARDS via activation of the Trx2/Myo19/Drp1 pathway. *J Pharm Anal*. 2025;15(3):101039. doi:10.1016/j.jpha.2024.101039

18. Bai XY, Liu P, Chai YW, et al. Artesunate attenuates 2,4-dinitrochlorobenzene-induced atopic dermatitis by down-regulating Th17 cell responses in BALB/c mice. *Eur J Pharmacol*. 2020;874:173020. doi:10.1016/j.ejphar.2020.173020
19. Radyuk SN. Mechanisms underlying the biological effects of molecular hydrogen. *Curr Pharm Des*. 2021;27(5):626–735. doi:10.2174/1381612826666201211112846
20. Li X, Li L, Liu X, et al. Attenuation of cardiac ischaemia-reperfusion injury by treatment with hydrogen-rich water. *Curr Mol Med*. 2019;19 (4):294–302. doi:10.2174/1566524019666190321113544
21. Ohsawa I. Biological responses to hydrogen molecule and its preventive effects on inflammatory diseases. *Curr Pharm Des*. 2021;27(5):659–666. doi:10.2174/1381612826666200925123510
22. Iketani M, Ohsawa I. Molecular hydrogen as a neuroprotective agent. *Curr Neuropharmacol*. 2017;15(2):324–331. doi:10.2174/1570159X14666160607205417
23. Zhang X, Yu P, Hong N, et al. Effect and mechanism of hydrogen-rich bath on mice with imiquimod-induced psoriasis. *Exp Dermatol*. 2023;32 (10):1674–1681. doi:10.1111/exd.14872
24. Fang W, Tang L, Wang G, et al. Molecular Hydrogen Protects Human Melanocytes from Oxidative Stress by Activating Nrf2 Signaling. *J Invest Dermatol*. 2020;140(11):2230–2241. doi:10.1016/j.jid.2019.03.1165
25. Banu J, Varela E, Guerra JM, et al. Dietary coral calcium and zeolite protects bone in a mouse model for postmenopausal bone loss. *Nutr Res*. 2012;32(12):965–975. doi:10.1016/j.nutres.2012.09.009
26. Madamsetty VS, Mohammadinejad R, Uzieliene I, et al. Dexamethasone: insights into pharmacological aspects, therapeutic mechanisms, and delivery systems. *ACS Biomater Sci Eng*. 2022;8(5):1763–1790. doi:10.1021/acsbiomaterials.2c00026
27. Qi B, Yu Y, Wang Y, Wang Y, Yu Y, Xie K. Perspective of molecular hydrogen in the treatment of sepsis. *Curr Pharm Des*. 2021;27(5):667–678. doi:10.2174/1381612826666200909124936
28. Quan L, Zheng B, Zhou H. Protective effects of molecular hydrogen on lung injury from lung transplantation. *Exp Biol Med*. 2021;246 (12):1410–1418. doi:10.1177/15353702211007084
29. Li Y, Li G, Suo L, Zhang J. Recent advances in studies of molecular hydrogen in the treatment of pancreatitis. *Life Sci*. 2021;264:118641. doi:10.1016/j.lfs.2020.118641
30. Tian Y, Zhang Y, Wang Y, et al. Hydrogen, a novel therapeutic molecule, regulates oxidative stress, inflammation, and apoptosis. *Front Physiol*. 2021;12:789507. doi:10.3389/fphys.2021.789507